

EPR Insensitivity of the Metal-Nitrosyl Spin-Bearing Moiety in Complexes $[\text{L}_n\text{Ru}^{\text{II}}\text{-NO}]^k$

Stéphanie Frantz,^[a] Biprajit Sarkar,^[a] Monika Sieger,^[a] Wolfgang Kaim,^{*,[a]}
Federico Roncaroli,^[b] José A. Olabe,^{*,[b]} and Stanislav Zális^[c]

Keywords: Density functional calculations / EPR spectroscopy / Nitric oxide / Radical complexes / Ruthenium

A survey of 18 paramagnetic species $[\text{L}_n\text{Ru}(\text{NO})]^k$, including seven new examples studied by in situ electrolysis, reveals a surprisingly narrow range of EPR parameters despite a wide variety of ligands such as pyridine, polypyridines, imines, amines, nitriles, phosphanes, carbonyl, cyclopentadienides, halides, hydride, hydroxide, thiocyanate or cyanide: $g_1 = 2.015 \pm 0.02$, $g_2 = 1.990 \pm 0.015$, $g_3 = 1.892 \pm 0.03$, $g_{\text{av}} = 1.968 \pm 0.02$, $\Delta g = g_1 - g_3 = 0.122 \pm 0.037$, $A_2(^{14}\text{N}) = 3.3 \pm 0.5$ mT. This rather small variability, smaller still if the organometallic compounds are excluded, differs from the wider range of EPR data reported for nitrosyliron species with $S = 1/2$; appar-

ently, the $\{\text{RuNO}\}^7$ configuration involves a rather invariant and relatively covalent metal–NO interaction. DFT calculations were employed for $[(\text{NC})_5\text{Ru}(\text{NO})]^{3-}$ to reproduce the EPR data, to evaluate the spin distribution (58% spin density on NO), and to reveal structural changes on reduction such as the Ru–N–O bending and Ru–NO bond lengthening. In addition, the possibility of staggered and eclipsed conformations is discussed.

(© Wiley-VCH Verlag GmbH & Co. KGaA, 69451 Weinheim, Germany, 2004)

Introduction

The formation, reactivity, spectroscopy and structures of nitrosyliron complexes have been investigated for more than a century.^[1–3] The question of the appropriate electronic description of such species in terms of oxidation and spin states has been highlighted recently by the examples of simple $[(\text{H}_2\text{O})_5\text{Fe}(\text{NO})]^{2+}$,^[4] of complexes $[(\text{L})\text{Fe}(\text{NO})]^{n+}$ with multidentate N-, S- or O-donor ligands L,^[5] and of nitrosyliron porphyrins inside or outside of heme proteins.^[6,7] Various iron oxidation states, from $-\text{II}^{[8]}$ to $+\text{IV}^{[9]}$ can be discussed in conjunction with nitrosonium (NO^+), nitric oxide (NO^\bullet) or nitroside (NO^-) ligands.^[10] Paramagnetic neutral NO^\bullet is of particular interest, and its presence has been observed frequently by vibrational or EPR spectroscopy.^[11–13]

The current surge in such studies is attributed to the recognition of the essential role of iron–NO interactions in a

physiological context,^[13] including the formation,^[14] binding, and release^[15] of this ubiquitous messenger (neurotransmitter) molecule.^[16] Copper^[17] or iron-coordinated NO also play an important role in the biological nitrogen cycle.^[18] In yet another line of interest, the metal-influenced chemistry of NO is of relevance for catalytic exhaust-gas conversion.^[19]

Recently, corresponding compounds of the higher homologue ruthenium have also been studied in the search for NO-scavenging^[20] or NO-releasing (delivering) agents.^[14,15,21] Scavenging by specifically designed ruthenium(III) aqua complexes containing polycarboxylate co-ligands was reported recently to involve a fast NO coordination, leading to formally $\text{Ru}^{\text{II}}(\text{NO}^+)$ complexes. However, the potential $\text{Ru}^{\text{II}}(\text{NO}^\bullet)$ product accessible by electrochemically reversible reduction^[20c] was not studied further.^[20a]

Photochemical or electron-transfer activation can be envisaged for the labilization of bound NO from its usual, kinetically stable $\text{Ru}^{\text{II}}(\text{NO}^+) = \{\text{RuNO}\}^6$ configuration.^[21] Following more recent assumptions^[22] on the transition from $\text{Ru}^{\text{II}}-(\text{NO}^+)$ to $\text{Ru}^{\text{II}}-(\text{NO}^\bullet)$ some EPR data on chemically generated $\text{Ru}^{\text{II}}(\text{NO}^\bullet)$ species and pertinent quantum-chemical calculations have been published in the last few years.^[21b,23–30] Herein we describe EPR results from the in situ reduction of several more such complexes $[\text{L}_n\text{Ru}(\text{NO})]^k$, we summarize and critically discuss the data of 18 different such species and compare the unexpectedly

^[a] Institut für Anorganische Chemie, Universität Stuttgart, Pfaffenwaldring 55, 70550 Stuttgart, Germany
E-mail: kaim@iac.uni-stuttgart.de

^[b] Departamento de Química Inorgánica, Analítica y Química Física, (INQUIMAE), Facultad de Ciencias Exactas y Naturales, UBA, Pabellón 2, Ciudad Universitaria, C1428EHA Buenos Aires, Republic of Argentina
E-mail: olabe@qi.fcen.uba.ar

^[c] J. Heyrovský Institute of Physical Chemistry, Academy of Sciences of the Czech Republic, Dolejškova 3, 18223 Prague, Czech Republic
E-mail: stanislav.zalis@jh-inst.cas.cz

uniform result with the situation in corresponding iron complexes. Results for the reduction and oxidation of $[Cl_5Ru(NO)]^{2-}$ are also presented, as are improved DFT calculations of the g and hyperfine properties of $[(NC)_5Ru(NO)]^{3-}$, including their orientation dependence (eclipsed vs. staggered conformation).

Results and Discussion

Although the new $Ru^{II}-(NO^+)$ precursor complexes referred to in the Exp. Sect. are reduced reversibly at room temperature, no EPR signals were detectable for the one-electron-reduced forms under those conditions. EPR silence at room temperature has been reported before for the related species from Table 1.^[22–25] In glassy frozen solution a typical pattern^[17,23–30] of rhombic g splitting with ^{14}N nitrosyl hyperfine coupling of the central component emerges, a representative spectrum from the in situ electrolysis of a precursor, $[(terpy)(bpz)Ru(NO)]^{3+}$, in $CH_3CN/0.1$ M Bu_4NPF_6 , is shown together with a computer simulation in Figure 1.

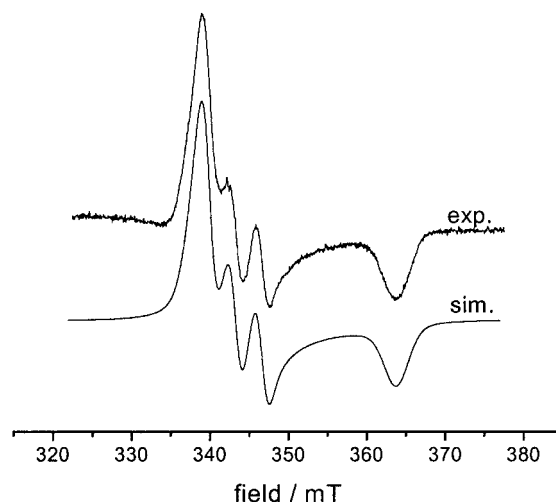


Figure 1. EPR spectrum of $[(terpy)(bpz)Ru(NO)]^{2+}$ at 110 K in $CH_3CN/0.1$ M Bu_4NPF_6 (top); computer simulation (bottom)

Conversion of commercially available $K_2[Cl_5Ru(NO)]$ into its tetrabutylammonium salt allowed us to additionally study its reduction behavior in acetonitrile. Even at -40 °C the electrochemical reduction proved to be irreversible,

Table 1. EPR spectroscopic data^[a] of nitrosylruthenium complexes; n.o. not observed

Complex	g_1	g_2	g_3	g_{av}	Δg	A_1	A_2	A_3	Ref.
$[(py)_4(NH_3)Ru(NO)]^{2+}$	2.0215	1.9875	1.878	1.963	0.1435	n.o.	3.0	n.o.	this work ^[b]
$[(py)_4(SCN)Ru(NO)]^+$	2.0225	1.9895	1.877	1.963	0.1455	n.o.	2.9	n.o.	this work ^[b]
$[(py)_4ClRu(NO)]^+$	2.025	1.990	1.886	1.967	0.139	n.o.	3.1	n.o.	this work ^[b]
$[(py)_4ClRu(NO)]^+$	2.033	1.989	1.874	1.965	0.159	1.51	3.18	1.07	[28][c]
$[(py)_4(OH)Ru(NO)]^+$	2.0235	1.991	1.886	1.967	0.1375	n.o.	3.2	n.o.	this work ^[b]
$[(bpy)_2(CH_3CN)Ru(NO)]^{2+}$	2.028	1.9925	1.882	1.968	0.146	n.o.	3.3	n.o.	this work ^[b]
$[(bpy)_2ClRu(NO)]^+$	2.029	1.992	1.881	1.968	0.148	n.o.	3.2	n.o.	this work ^[b]
$[(terpy)(bpy)Ru(NO)]^{2+}$	2.0175	1.998	1.883	1.967	0.1345	n.o.	3.4	n.o.	this work ^[b]
$[(terpy)(bpz)Ru(NO)]^{2+}$	2.0215	1.999	1.886	1.969	0.1355	n.o.	3.4	n.o.	this work ^[b]
$[(NC)(py)_4Ru(\mu-CN)(py)_4Ru(NO)]^{2+}$	2.024	1.990	1.865	1.960	0.159	1.55	3.39	0.97	[28][c]
$[(cyclam)ClRu(NO)]^+$	2.035	1.995	1.883	1.971	0.152	1.7	3.21	1.5	[24,25b][d]
$[(bpydip)ClRu(NO)]^+$	2.027	1.991	1.889	1.969	0.138	1.69	3.23	1.48	[29][e]
$[(dppe)_2ClRu(NO)]^+$	2.011	1.976	1.867	1.951	0.144	1.71	1.85 ^[f]	1.43	[25b][g]
$[(depe)_2ClRu(NO)]^+$	2.010	1.984	1.888	1.961	0.122	1.8	3.5	1.9	[25b][d]
$[(NC)_5Ru(NO)]^{3-}$	2.004	2.002	1.870	1.959	0.134	n.o.	3.8	n.o.	[27][h]
$[(Ph_3P)_2(C_5Me_5)Ru(NO)]^+$	2.0115	1.983	1.900	1.965	0.111	1.63	2.10 ^[f]	2.29	[30a][i]
	1.995	1.995	1.896	1.962	0.099	n.o.	2.85	n.o.	[30a][j]
$[(PhMe_2P)_2(C_5Me_5)Ru(NO)]^+$	2.000	1.998	1.915	1.970	0.085	1.06	3.38	1.07	[30a][i]
	1.996	1.996	1.964 ^[f]	1.985 ^[f]	0.032 ^[f]	n.o.	3.25	n.o.	[30a][j]
$[(Me_3P)_2(C_5Me_5)Ru(NO)]^+$	2.007	2.002	1.918	1.976	0.089	1.15	3.37	1.20	[30a][i]
	2.001	1.994	1.912	1.969	0.089	0.6	3.3	1.3	[30a][j]
$[HCl(OC)(P^iPr_3)_2Ru(NO)]$	2.006	1.993	1.910	1.970	0.096	n.o.	3.45	n.o.	[30b][k]
$[DCl(OC)(P^iPr_3)_2Ru(NO)]$	2.001	1.994	1.910	1.968	0.091	n.o.	3.45	n.o.	[30b][k]

[a] ^{14}N hyperfine coupling A in mT. [b] In $CH_3CN/0.1$ M Bu_4NPF_6 , measured at 110 K. [c] In $CH_3CN/0.1$ M Bu_4NPF_6 , measured at 10 K. [d] In ethylene glycol + 30% H_2O , measured at 77 K; cyclam = 1,4,8,11-tetraazacyclotetradecane; depe = 1,2-bis(diethylphosphanyl)ethane. [e] In CH_3CN , measured at 110 K; bpydip = N,N' -bis(7-methyl-2-pyridylmethylene)-1,3-diiminopropane. [f] Probably erroneous value. [g] In CH_2Cl_2 , measured at 77 K; dppe = 1,2-bis(diphenylphosphanyl)ethane. [h] In $CH_3CN/0.1$ M Bu_4NPF_6 , measured at 3.5 K. [i] In CH_2Cl_2 , measured at 113 K. [j] In acetone, measured at 100 K. [k] In toluene, measured at 77 K. Additional 1H hyperfine coupling observed at about 3.5 mT.

presumably due to the facile dissociation of chloride. In contrast, reversible oxidation produced a species with an EPR signal ($g_{1,2} = 2.1075$, $g_3 = 2.0577$) which will have to be analyzed further.

The results for the reversibly reduced systems are summarized, together with literature data, in Table 1; most previously reported species were obtained by chemical reduction with, for example, Zn/Hg^[29] or Eu²⁺.^[21b,24,25b]

The spectra reported here were simulated without incorporating unresolved nitrosyl ¹⁴N hyperfine splitting of the g_1 and g_3 components. Such incorporation has been reported in the literature;^{[25,29][30b]} however, the corresponding values between 1 and 2 mT, or even below, may rather serve as an approximation or upper limit and they will not be discussed further. Accuracy of the g factors is assumed to be ± 0.0005 (g_1), ± 0.0002 (g_2) and ± 0.001 (g_3); the A_2 values are given with a ± 0.1 mT error margin.

Given the wide variety of ligands L for the species $[L_nRu(NO)]^k$ in Table 1 (L = pyridine, polypyridines, imines, amines, nitriles, phosphanes, carbonyl, cyclopentadienide, halides, hydride, hydroxide, thiocyanate, cyanide), the small degree of EPR parameter variation is surprising:

$g_1 = 2.015 \pm 0.02$, $g_2 = 1.990 \pm 0.015$, $g_3 = 1.892 \pm 0.03$, $g_{av} = 1.968 \pm 0.02$, $\Delta g = g_1 - g_3 = 0.122 \pm 0.037$, $A_2(^{14}N) = 3.3 \pm 0.5$ mT.

The variance is still smaller if organometallic derivatives^[30] are excluded.

Paramagnetic nitrosyliron complexes, even those involving only low-spin systems,^[4,5,7,31] exhibit a distinctly greater variation. In part this may reflect contributions from the more accessible valence-tautomeric $M^I(NO^+)$ state for $M = Fe$ which has a $(d_x^2)^1$ configuration and leads to $g_{1,2} \approx 2.07$, $g_3 \approx 2.0$ and $g_{av} \approx 2.03$ for clearly established $Fe^I(NO^+)$ cases.^[25,31b]

On average, the g anisotropy, $\Delta g = g_1 - g_3$, is about twice as large for the ruthenium complexes as for related nitrosyliron(II) species.^[27] This is an immediate consequence of the higher spin-orbit coupling constant $\xi(Ru) \approx 2\xi(Fe)$.^[32] The deviation of g from the free-electron value of 2.0023 results from admixtures of higher excited states with nonzero angular momentum; according to the approximation in Equation (1) the spin-orbit coupling constant, ξ , is a crucial factor.^[33]

$$g = g_e - \frac{2}{3} \sum_i \sum_n \sum_{kj} \frac{\langle \psi_0 | \xi_k L \delta_k | \psi_n \rangle \langle \psi_n | L_{ij} \delta_j | \psi_0 \rangle}{E_n - E_0} = g_e + \Delta g \quad (1)$$

ξ : spin orbit coupling constant

L : angular momentum operator

E_0 : energy of singly occupied molecular orbital (SOMO)

Unrestricted ADF/BP calculations for the most symmetric species $[(NC)_5Ru(NO)]^{3-}$ have confirmed the expected^[11] and recently experimentally confirmed^[30b] bending of the RuNO moiety to 146.1° [$138.75(11)^\circ$ for

$[HCl(OC)(PiPr_3)_2Ru(NO)]^{[30b]}$ and the lengthening of the Ru–NO bond by 0.128 \AA to 1.899 \AA [$1.8566(11) \text{ \AA}$ for $[HCl(OC)(PiPr_3)_2Ru(NO)]^{[30b]}$], in agreement with the established NO labilization on reduction for potential medical applications.^[20,21] G98/B3LYP calculations give an RuNO angle of 146.7° and a Ru–NO bond length of 1.915 \AA . ADF/SAOP calculations indicated about 29% metal and 58% NO contributions to the singly occupied molecular orbital (SOMO), suggesting $Ru^{II}-(NO^\cdot)$ as the dominant oxidation state formulation, albeit with considerable mixing.^[27] The lowest (completely) unoccupied molecular orbital (LUMO) is the second NO-based π^* MO (25% metal and 62% NO contribution), originating from the degenerate e level of $[(NC)_5Ru(NO)]^{2-}$. The calculated values (g_n , A_n) are listed in Table 2.

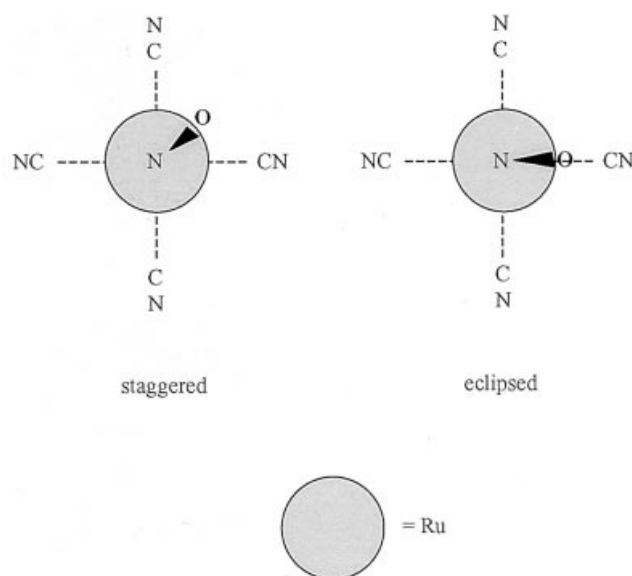
Table 2. Comparison of experimental and calculated g values and hyperfine constants A (mT) for $[(NC)_5Ru(NO)]^{3-}$ at optimized geometry (eclipsed conformation)

	Exp.	Calcd. ^[a]	Calcd. ^[b]	Calcd. ^[c]
g_1	2.004	2.000	2.006	2.007
g_2	2.002	1.993	1.996	1.997
g_3	1.870	1.814	1.845	1.890
$g_1 - g_3$	0.134	0.186	0.161	0.117
$g_{iso}^{[d]}$	1.959	1.936	1.949	1.965
$A_1(^{101}Ru)$	n.o.	0.96	–	1.13
$A_2(^{101}Ru)$	n.o.	1.61	–	1.67
$A_3(^{101}Ru)$	n.o.	0.24	–	0.46
$A_1(^{14}N)$	n.o.	0.51	–	1.28
$A_2(^{14}N)$	3.8	3.23	–	4.04
$A_3(^{14}N)$	n.o.	0.35	–	1.14

^[a] ADF/BP calculations: g values calculated using spin-restricted approach including spin-orbit coupling; A values calculated within the UKS-ZORA approach with core electrons included. ^[b] ADF/SAOP spin-restricted ZORA calculations including spin-orbit coupling. ^[c] UKS-Pauli approach. ^[d] Calculated from $\langle g \rangle = [(g_1^2 + g_2^2 + g_3^2)/3]^{1/2}$.

The well-known bending of the M–N–O moiety in $\{MNO\}^7$ species with approximately octahedral configuration at M produces a conformational isomerism characterized by variations of the C(CN)–Ru–N–O dihedral angle, θ , with the eclipsed ($\theta = 0^\circ$) and staggered ($\theta = 45^\circ$) conformations as the two extreme cases (Scheme 1). G98/B3LYP geometry optimization shows the eclipsed conformation to be more stable by 0.041 eV (as in $[HCl(OC)(PiPr_3)_2Ru(NO)]^{[30b]}$), the rotational barrier being highly dependent on the functional used. The calculated g_n , $A_n(^{14}N)$ and $A_n(^{101}Ru)$ parameters depend only slightly on the conformation.

The analysis of individual contributions to the Δg values was performed within the UKS-Pauli approach, indicating that the largest contribution arises from the paramagnetic orbital-orbital coupling between the SOMO and LUMO of the same spin polarization. The experimental g values are well reproduced by the calculations. Table 2 shows how the functional and the type of approach influence the calculated values. The best agreement between experimental and calculated g values was achieved using either the ADF/



Scheme 1

SAOP spin-restricted ZORA spin-orbit calculation or the UKS-Pauli approach.

The spin distribution in complexes $[L_nRu(NO)]^k = \{RuNO\}^7$ seems to be rather invariant throughout the complexes of Table 1, reflecting the high degree of covalency of the Ru–N bond in the $\{RuNO\}^{17}$ configuration with 19 valence electrons. Increasing covalency is also responsible for the general shift to higher g values on going from Na^+-NO^\bullet via Cu^I complexes^[34] to the Ru^{II} compounds summarized here. In comparison to the results given here, some other calculations^[26,29] seem to underestimate the NO contributions. In that context, some conclusions based on very small $\nu(NO)$ shifts on reduction such as a $Ru^{III}(NO^\bullet)$ formulation for $[(cyclam)ClRu(NO)]^{2+}$ or a ligand-delocalized description $(L^-)Ru^{II}(NO^+)$ suggested for $[(bpydip)ClRu(NO)]^+$ ^[29] are not supported by the EPR data [$cyclam = 1,4,8,11$ -tetraazacyclotetradecane; $bpydip = N,N'$ -bis(7-methyl-2-pyridylmethylene)-1,3-diminopropane].

Despite the rather uniform EPR results for the species in Table 1 there are some slight variations. The most symmetrical species $[(NC)_5Ru(NO)]^{3-}$ displays a g component splitting approaching the axial limit, with $g_\perp > g_\parallel$. The average value of g is smallest for this species whereas it is slightly larger (in 0.012) for $[(cyclam)ClRu(NO)]^+$; however, all $Ru^{II}(NO^\bullet)$ complexes have g_{av} below 2, indicating the closeness of both π^* orbitals of NO^{27} and thus of both $^2\Pi_x$ and $^2\Pi_y$ states.^[34,35] The presence of states lying close to the radical ground state is also responsible for the rapid relaxation as evident from the EPR silence at room temperature. The relatively large A_2 hyperfine value of 3.8 mT for $^{14}N(NO)$ may in part reflect the reluctance of negatively charged cyanide ligands in $[(NC)_5Ru(NO)]^{3-}$ to accommodate the unpaired electron. On the other hand, the A_2 values are smallest, at about 3.0 mT, for the series of complexes $[(py)_4XRu(NO)]^+$ with rather weak donor ligands (Table 1).

The total g anisotropy $\Delta g = g_1 - g_3$ is highest for the dinuclear complex $[(NC)(py)_4Ru(CN)(py)_4Ru(NO)]^{2+}$, possibly reflecting an effect of the second, non-NO-coordinating metal center with its high spin-orbit coupling constant. $[(NC)_5Ru(NO)]^{3-}$ and the phosphane-containing compound $[(depe)_2ClRu(NO)]^+$ [$depe = 1,2$ -bis(diethylphosphanyl)ethane], both with strong σ donor/ π acceptor ligation, display relatively small Δg values, indicating smaller metal contributions; this is also supported by rather high nitrosyl ligand coupling constants $A_2(^{14}N)$.

Changing the solvent from CH_3CN to DMF in the case of $[(py)_4ClRu(NO)]^+$ yielded identical EPR parameters. Although the cyanoiron compounds $[(NC)_5Fe(L)]^{2-}$ [$L = NO^+$ or N -methylpyrazinium (mpz)] can lose one cyanide ligand on reduction^[36,37] we found no evidence for conversion into a five-coordinate complex in the paramagnetic ruthenium species studied here. The new calculated metal hyperfine coupling constants $A_n(^{101}Ru)$ (Table 2) confirm the failure to observe such splittings experimentally. Even the calculated A_2 value of 1.61 mT would be difficult to detect because of the line-width, the relatively low natural abundance of only 17% and the distribution of signal intensity over six lines ($I = 5/2$). The isotope ^{99}Ru (12.7% natural abundance, $I = 5/2$) has a 10% smaller hyperfine coupling^[45] and would be still harder to detect. The maximum calculated isotropic hyperfine splitting of 0.94 mT according to Table 2 is only slightly larger than the $A_{iso}(^{101}Ru)$ parameters measured for radical complexes containing cyanoruthenium^[37,38] (≤ 0.52 mT) or other ruthenium(II) complex fragments (≤ 0.86 mT).^[39] Species with metal-centered spin containing ruthenium(II)^[40] are expected to have isotropic metal coupling constants of several milliteslas.

In summary, the small variation in g tensor splitting and hyperfine coupling for all 18 compounds in Table 1 suggest very similar electronic structures, described essentially by the $Ru^{II}(NO^\bullet)$ formulation. The surprising invariance of EPR parameters points to a higher degree of covalency in the $\{RuNO\}^7$ situation than in the corresponding $\{FeNO\}^7$ arrangements, the latter having more accessible options between the limiting structures $Fe^{II}(NO^\bullet)$ and $Fe^I(NO^+)$ and between low-spin and high-spin states. Perspectives for future work will include nitrosylruthenium complexes with strongly dominant co-ligands such as porphyrins or other macrocycles^[41] and the study of osmium analogues with their much higher spin-orbit coupling contributions from the 5d metal.

Experimental Section

Instrumentation: IR spectra were recorded with KBr pellets on a Thermo Nicolet model Avatar 320 FT-IR instrument. 1H NMR spectra were obtained on a Bruker 500 MHz spectrometer. Electrochemical studies were performed with a Princeton Applied Research potentiostat 273A, by square-wave voltammetry (SWV) at 60 Hz, with vitreous carbon as working electrode and $Ag/AgCl$ (3 M KCl) as reference. The electrolyte was an aqueous solution that was 1 M in NaCl and 0.01 M in HCl. Elemental analyses were done on a Carlo Erba elemental analyser, model 1106. EPR spec-

troscopy: The nitrosylruthenium complexes were reduced for in situ EPR studies in a two-electrode capillary described earlier.^[42] The electrolyte was CH₃CN/0.1 M Bu₄NPF₆. Whereas the brief (ca. 10 min) electrolysis was performed at 295 K, the EPR spectra were recorded at 110 K in glassy frozen solutions due to the EPR silence of the complexes at room temperature. A Bruker ESP 300 spectrometer was used. The *g* factor determination was carried out with a Bruker ER035M gaussmeter and a HP 5350B microwave counter. The spectra were simulated (program Bruker WinSimfonia) without incorporating the unresolved hyperfine splitting of the *g*₁ and *g*₃ components.

The complexes *trans*-[(py)₄ClRu(NO)](PF₆)₂,^[43] *trans*-[(py)₄(OH)Ru(NO)](PF₆)₂,^[43] *trans*-[(py)₄(NH₃)Ru(NO)](BF₄)₃,^[44a] *cis*-[(bpy)₂ClRu(NO)](PF₆)₂,^[23] *cis*-[(bpy)₂(CH₃CN)Ru(NO)](PF₆)₂^[44b] and [(terpy)(bpy)Ru(NO)](PF₆)₃^[45] were prepared as described previously.

[(terpy)(bpz)Ru(NO)](PF₆)₃: [RuCl₃(terpy)]^[46] (100 mg, 0.227 mmol) and bpz (2,2'-bipyrazine, 60 mg, 0.379 mmol) were heated to reflux for 3 h in 50 mL of EtOH/H₂O (1:1). NaNO₂ (150 mg) was added to the red-brown solution and refluxing was continued for 2 h. The red solution was then filtered and a concentrated solution of NH₄PF₆ was added until complete precipitation of the product was ensured. The red solid was suspended in 3 M HCl and NH₄PF₆ was added in the same way as before to afford a brown solid. The product was further purified by recrystallization from acetonitrile/diethyl ether. IR: $\nu(\text{NO}) = 1957 \text{ cm}^{-1}$. $E_{1/2} = 0.46 \text{ V}$ vs. Ag/AgCl. C₂₈H₁₇F₁₈N₈O₃P₃Ru (957.40): calcd. C 28.85, N 1.79, N 11.71; found C 27.66, N 1.74, N 11.04. ¹H NMR (CD₃CN): $\delta = 10.12$ (s, 1 H), 9.96 (s, 1 H), 9.51 (d, 1 H), 9.38 (d, 1 H), 8.99 (t, 1 H), 8.87 (d, 2 H), 8.82 (d, 1 H), 8.71 (d, 2 H), 8.47 (t, 2 H), 8.06 (d, 2 H), 7.73 (t, 2 H), 7.22 (t, 1 H) ppm.

***trans*-[(py)₄(SCN)Ru(NO)](PF₆)₂:** *trans*-[(py)₄Ru(NO₂)₂]^[43] (100 mg, 0.0106 mmol) and NaSCN (300 mg, 3.7 mmol) were suspended in 20 mL of acetonitrile, and 0.5 mL of concentrated HPF₆ was added. After mixing, the sample was evaporated to dryness. The solid residue was suspended in water and filtered. 700 mg of NH₄PF₆ was added to the solution and a yellow solid was obtained. This compound was further purified by loading onto a DOWEX 50 WX2 cation exchanger (100–200 mesh) in acid form eluting with 1 M HCl. The main orange fraction was collected and precipitated with NH₄PF₆. C₂₁H₂₀F₁₂N₆O₂P₂RuS (795.49): calcd. C 31.69, H 2.01, N 10.56, S 4.03; found C 31.90, H 2.27, N 10.12, S 3.63. IR: $\nu(\text{NO}) = 1902 \text{ cm}^{-1}$. $E_{1/2} = 0.12 \text{ V}$ and -0.35 V vs. Ag/AgCl. ¹H NMR (CD₃CN): $\delta = 8.29$ (t, 4 H, H⁴), 8.26 (d, 8 H, H^{2,6}), 7.70 (t, 8 H, H^{3,5}) ppm.

DFT Calculations: Ground state electronic structure calculations on [(NC)₅Ru(NO)]³⁻ have been done on the basis of density-functional theory (DFT) methods using the ADF2002.03^[47,48] and Gaussian 98 program packages.^[49]

Within the ADF program, Slater-type orbital (STO) basis sets of triple-quality with polarization functions were employed. Basis I was represented by the frozen-core approximation (1s for C, N O and 1s–3d for Ru), basis II also includes core electrons. The following density functionals were used within ADF: the local density approximation (LDA) with VWN parametrization of electron gas data or the functional including Becke's gradient correction^[50] to the local exchange expression in conjunction with Perdew's gradient correction^[51] to the LDA expression (ADF/BP). The scalar relativistic (SR) zero-order regular approximation (ZORA) was used within the geometry optimization. The *g*-tensor calculations were also performed using the asymptotically correct functional SAOP (statistical average of orbital potentials),^[52] which gives better ener-

gies of the frontier MOs. Core electrons were included in the ADF/SAOP calculations.

The *g*-tensor was obtained from a spin-nonpolarized wave function after incorporating the spin-orbit (SO) coupling. *A* tensors and *g* tensors were obtained by first-order perturbation theory from the ZORA Hamiltonian in the presence of a time-independent magnetic field.^[53,54] The analysis of individual contributions to the *g* tensor was done by the UKS-Pauli approach using gauge-including atomic orbitals.^[55]

Within Gaussian-98 Dunning's polarized valence double- ζ basis sets^[56] were used for the C, N and O atoms and the quasi-relativistic effective core pseudopotentials with a correspondingly optimized set of basis functions^[57] for Ru. The hybrid Becke three-parameter functional with Lee, Yang and Parr correlation functional (B3LYP)^[58] was used in the Gaussian-98 calculations (G98/B3LYP).

The geometry of [(NC)₅Ru(NO)]³⁻ was optimized without any symmetry restrictions using the spin-unrestricted open-shell Kohn–Sham (UKS) approach.

Acknowledgments

This work was supported by a grant from Volkswagenstiftung (I/76674), by the FCI, the European Union (COST action D14), the Ministry of Education of the Czech Republic (grant COST OC14.20), and by the Argentine Agencies CONICET and FONCYT (Grant 06–06817).

- [1] [1a] L. Playfair, *Proc. Roy. Soc., (London)* **1849**, 5, 846. [1b] L. Playfair, *Ann. Pharm.* **1850**, 74, 317.
- [2] J. H. Swinehart, *Coord. Chem. Rev.* **1967**, 2, 385.
- [3] [3a] J. A. McCleverty, *Chem. Rev.* **1979**, 79, 53. [3b] R. D. Feltham, J. H. Enemark, *Top. Stereochem.* **1981**, 12, 155.
- [4] A. Wanat, T. Schnepfensieper, G. Stochel, R. van Eldik, E. Bill, K. Wieghardt, *Inorg. Chem.* **2002**, 41, 4.
- [5] [5a] M. Li, D. Bonnet, E. Bill, F. Neese, T. Weyhermüller, N. Blum, D. Sellmann, K. Wieghardt, *Inorg. Chem.* **2002**, 41, 3444. [5b] T. Schnepfensieper, A. Wanat, G. Stochel, S. Goldstein, D. Meyerstein, R. van Eldik, *Eur. J. Inorg. Chem.* **2001**, 2317.
- [6] [6a] B. A. Averill, *Chem. Rev.* **1996**, 96, 2951. [6b] N. S. Trofimova, A. Y. Safronov, O. Ikeda, *Inorg. Chem.* **2003**, 42, 1945, and references cited therein.
- [7] [7a] W. R. Scheidt, M. K. Ellison, *Acc. Chem. Res.* **1999**, 32, 350. [7b] B. B. Wayland, L. W. Olson, *J. Am. Chem. Soc.* **1974**, 96, 6037. [7c] Y. Chen, M. A. Sweetland, R. E. Shepherd, *Inorg. Chim. Acta* **1997**, 260, 163.
- [8] [8a] C. Couture, J. R. Morton, K. F. Preston, S. J. Strach, *J. Magn. Reson.* **1980**, 41, 88. [8b] H. tom Dieck, H. Bruder, E. Köhl, D. Junghans, K. Hellfeldt, *New. J. Chem.* **1989**, 13, 259.
- [9] C. Hauser, T. Glaser, E. Bill, T. Weyhermüller, K. Wieghardt, *J. Am. Chem. Soc.* **2000**, 122, 4352.
- [10] [10a] J. A. Olabe, L. Slep, *Comprehensive Coordination Chemistry II* (Eds.: J. A. McCleverty, T. J. Meyer), Pergamon, **1993**, vol. 1, p. 603–623. [10b] J. A. Olabe, *Adv. Inorg. Chem.*, in press.
- [11] J. H. Enemark, R. D. Feltham, *Coord. Chem. Rev.* **1974**, 13, 339.
- [12] G. B. Richter-Addo, P. Legzdins, *Metal Nitrosyls*, Oxford University Press, New York, **1992**.
- [13] *Methods in Nitric Oxide Research* (Eds.: M. Feelisch, J. S. Stamler), Wiley, Chichester, **1996**.
- [14] P. C. Ford, I. M. Lorkovic, *Chem. Rev.* **2002**, 102, 993.
- [15] [15a] P. G. Wang, M. Xian, X. Tang, X. Wu, Z. Wen, T. Cai, A. Janczuk, *Chem. Rev.* **2002**, 102, 1091. [15b] J. A. Hrabie, L. K. Keefer, *Chem. Rev.* **2002**, 102, 1135.
- [16] F. Murad, *Angew. Chem. Int. Ed.* **1999**, 28, 1856.
- [17] C. E. Ruggiero, S. M. Carrier, W. E. Antholine, J. W. Whittaker,

- C. J. Cramer, W. B. Tolman, *J. Am. Chem. Soc.* **1993**, *115*, 11285.
- [18] S. J. Ferguson, *Curr. Opin. Chem. Biol.* **1998**, *2*, 182.
- [19] [19a] M. Iwamoto, H. Hamada, *Catal. Today* **1991**, *10*, 57. [19b] M. H. Groothaert, J. A. van Bokhoven, A. A. Battiston, B. M. Weckhuysen, R. A. Schoonheydt, *J. Am. Chem. Soc.* **2003**, *125*, 7629.
- [20] [20a] B. R. Cameron, M. C. Darkes, H. Yee, M. Olsen, S. P. Fricker, R. T. Skerlj, G. J. Bridger, N. A. Davies, M. T. Wilson, D. J. Rose, J. Zubieta, *Inorg. Chem.* **2003**, *42*, 1868. [20b] B. Serli, E. Zangrando, T. Gianferrara, L. J. Yellowlees, E. Alessio, *Coord. Chem. Rev.* **2003**, *245*, 73. [20c] M. R. Rhodes, M. H. Barley, T. J. Meyer, *Inorg. Chem.* **1991**, *30*, 629.
- [21] [21a] M. Wolak, R. van Eldik, *Coord. Chem. Rev.* **2002**, *230*, 263. [21b] E. Tfouni, M. Krieger, B. R. McGarvey, D. W. Franco, *Coord. Chem. Rev.* **2003**, *236*, 57.
- [22] [22a] S. S. S. Borges, C. U. Davanzo, E. E. Castellano, J. Z. Schpector, S. C. Silva, D. W. Franco, *Inorg. Chem.* **1998**, *37*, 2670. [22b] C. W. B. Bezerra, C. S. Silva, M. T. P. Gambardella, R. H. A. Santos, L. M. A. Plicas, E. Tfouni, D. W. Franco, *Inorg. Chem.* **1999**, *38*, 5660.
- [23] R. W. Callahan, T. J. Meyer, *Inorg. Chem.* **1977**, *16*, 574. The EPR spectrum of $[(bpy)_2ClRu(NO)]^+$ shown in this publication was not analyzed.
- [24] D. R. Lang, J. A. Davis, L. G. F. Lopes, A. A. Ferro, L. C. G. Vasconcellos, D. W. Franco, E. Tfouni, A. Wieraszko, M. J. Clarke, *Inorg. Chem.* **2000**, *39*, 2294.
- [25] [25a] R. C. L. Zampieri, G. Von Poelhsitz, A. A. Batista, O. R. Nascimento, J. Ellena, E. E. Castellano, *J. Inorg. Biochem.* **2002**, *92*, 82. [25b] B. R. McGarvey, A. A. Ferro, E. Tfouni, C. W. Brito Bezerra, I. Bagatin, D. W. Franco, *Inorg. Chem.* **2000**, *39*, 3577.
- [26] J. A. Gomez, D. Guenzburger, *Chem. Phys.* **2000**, *253*, 73.
- [27] M. Wanner, T. Scheiring, W. Kaim, L. D. Slep, L. M. Baraldo, J. A. Olabe, S. Zalis, E. J. Baerends, *Inorg. Chem.* **2001**, *40*, 5704.
- [28] F. Roncaroli, L. M. Baraldo, L. D. Slep, J. A. Olabe, *Inorg. Chem.* **2002**, *41*, 1930.
- [29] V. R. de Souza, A. M. de Costa Ferreira, H. E. Toma, *Dalton Trans.* **2003**, 458.
- [30] [30a] P. Diversi, M. Fontani, M. Fuligni, F. Laschi, F. Marchetti, S. Matteoni, C. Pinzino, P. Zanello, *J. Organomet. Chem.* **2003**, *675*, 21. [30b] A. V. Marchenko, A. N. Vedernikov, D. F. Dye, M. Pink, J. M. Zaleski, K. G. Caulton, *Inorg. Chem.* **2004**, *43*, 351.
- [31] [31a] J. D. W. van Voorst, P. J. Hemmerich, *Chem. Phys.* **1966**, *45*, 3914. [31b] N. Reginato, C. T. C. M. cCrory, D. Pervitsky, L. Li, *J. Am. Chem. Soc.* **1999**, *121*, 10217.
- [32] D. W. Pipes, T. J. Meyer, *Inorg. Chem.* **1984**, *23*, 2466.
- [33] W. Kaim, *Coord. Chem. Rev.* **1987**, *76*, 187.
- [34] K. M. Neyman, D. I. Ganyushin, V. A. Nasluzov, N. Rösch, A. Pöpl, M. Hartmann, *Phys. Chem. Chem. Phys.* **2003**, *5*, 2429.
- [35] P. Pietrzyk, W. Piskorz, Z. Sojka, E. Broclawik, *J. Phys. Chem. B* **2003**, *107*, 6105.
- [36] EPR of $[(NC)_4Fe(NO)]^{2-}$: C. Glidewell, I. L. Johnson, *Inorg. Chim. Acta* **1987**, *132*, 145.
- [37] E. Waldhör, W. Kaim, J. A. Olabe, L. D. Slep, J. Fiedler, *Inorg. Chem.* **1997**, *36*, 2969.
- [38] E. Waldhör, J. Poppe, W. Kaim, E. Cutin, M. Garcia Posse, N. E. Katz, *Inorg. Chem.* **1995**, *34*, 3093.
- [39] M. Krejcek, S. Zalis, J. Klima, D. Sykora, W. Matheis, A. Klein, W. Kaim, *Inorg. Chem.* **1993**, *32*, 3362.
- [40] C. Bianchini, F. Laschi, M. Peruzzini, P. Zanello, *Gazz. Chim. Ital.* **1994**, *124*, 271.
- [41] [41a] K. M. Kadish, V. A. Adamian, E. V. Caemelbecke, Z. Tan, P. Tagliatesta, P. Bianco, T. Boschi, G. Yi, M. A. Khan, G. Richter-Addo, *Inorg. Chem.* **1996**, *35*, 1343. [41b] K. M. Miranda, X. Bu, I. Lorkovic, P. C. Ford, *Inorg. Chem.* **1997**, *36*, 4838. [41c] D. S. Bohle, C. H. Hung, B. D. Smith, *Inorg. Chem.* **1998**, *37*, 5798. [41d] G. B. Richter-Addo, R. A. Wheeler, C. A. Hixson, L. Chen, M. A. Kahn, M. K. Ellison, C. E. Schulz, W. R. Scheidt, *J. Am. Chem. Soc.* **2001**, *123*, 6314. [41f] J. C. Patterson, I. M. Lorkovic, P. C. Ford, *Inorg. Chem.* **2003**, *42*, 4902.
- [42] W. Kaim, S. Ernst, V. Kasack, *J. Am. Chem. Soc.* **1990**, *112*, 173.
- [43] F. Bottomley, M. Mukaida, *J. Chem. Soc., Dalton Trans.* **1982**, 1933.
- [44] [44a] H. Nishimura, H. Matsuzawa, T. Togano, M. Mukaida, H. Kakihana, *J. Chem. Soc., Dalton Trans.* **1990**, 137. [44b] H. Nagao, K. Ito, N. Tsuboya, D. Ooyama, N. Nagao, S. F. Howell, M. Mukaida, *Inorg. Chim. Acta* **1999**, *290*, 113.
- [45] J. A. Weil, J. R. Bolton, J. E. Wertz, *Electron Paramagnetic Resonance*, Wiley, New York, **1994**.
- [46] C. A. Bessel, R. A. Leising, L. F. Szczepura, W. J. Perez, H. Vo, H. My, K. J. Takeuchi, *Inorg. Synth.* **1988**, *32*, 186.
- [47] G. te Velde, F. M. Bickelhaupt, S. J. A. van Gisbergen, C. Fonseca Guerra, E. J. Baerends, J. G. Snijders, T. Ziegler, *J. Comput. Chem.* **2001**, *22*, 931.
- [48] C. Fonseca Guerra, J. G. Snijders, G. te Velde, E. J. Baerends, *Theor. Chim. Acc.* **1998**, *99*, 391.
- [49] M. J. Frisch, G. W. Trucks, H. B. Schlegel, G. E. Scuseria, M. A. Robb, J. R. Cheeseman, V. G. Zakrzewski, J. A. Montgomery, Jr., R. E. Stratmann, J. C. Burant, S. Dapprich, J. M. Millam, A. D. Daniels, K. N. Kudin, M. C. Strain, O. Farkas, J. Tomasi, V. Barone, M. Cossi, R. Cammi, B. Mennucci, C. Pomelli, C. Adamo, S. Clifford, J. Ochterski, G. A. Petersson, P. Y. Ayala, Q. Cui, K. Morokuma, D. K. Malick, A. D. Rabuck, K. Raghavachari, J. B. Foresman, J. Cioslowski, J. V. Ortiz, A. G. Baboul, B. B. Stefanov, G. Liu, A. Liashenko, P. Piskorz, I. Komaromi, R. Gomperts, R. L. Martin, D. J. Fox, T. Keith, M. A. Al-Laham, C. Y. Peng, A. Nanayakkara, C. Gonzalez, M. Challacombe, P. M. W. Gill, B. Johnson, W. Chen, M. W. Wong, J. L. Andres, C. Gonzalez, M. Head-Gordon, E. S. Replogle, J. A. Pople, Gaussian 98, Revision A.11; Gaussian, Inc.: Pittsburgh, PA, **1998**.
- [50] A. D. Becke, *Phys. Rev. A* **1988**, *38*, 3098.
- [51] J. P. Perdew, *Phys. Rev. A* **1986**, *33*, 8822.
- [52] P. R. T. Schipper, O. V. Gritsenko, S. J. A. van Gisbergen, E. J. Baerends, *J. Chem. Phys.* **2000**, *112*, 1344.
- [53] E. van Lenthe, A. van der Avoird, P. E. S. Wormer, *J. Chem. Phys.* **1997**, *107*, 2488.
- [54] E. van Lenthe, A. van der Avoird, P. E. S. Wormer, *J. Chem. Phys.* **1998**, *108*, 4783.
- [55] G. Schrenkenbach, T. Ziegler, *J. Phys. Chem. A* **1997**, *101*, 3388.
- [56] D. E. Woon, T. H. Dunning Jr., *J. Chem. Phys.* **1993**, *98*, 1358.
- [57] D. Andrae, U. Häussermann, M. Dolg, H. Stoll, H. Preuss, *Theor. Chim. Acta* **1990**, *77*, 123.
- [58] P. J. Stephens, F. J. Devlin, C. F. Cabalowski, M. J. Frisch, *J. Phys. Chem.* **1994**, *98*, 11623.

Received January 16, 2004

Early View Article

Published Online May 13, 2004